R. & M. No. 2904
(13,567)
A.R.C. Technical Report

MINISTRY OF SUPPLY

AERONAUTICAL RESEARCH COUNCIL
REPORTS AND MEMORANDA

A Note on the Dynamic Stability of Aircraft at High-Subsonic Speeds when Considering Unsteady Flow

By
W. J. G. PINSKER

LONDON: HER MAJESTY'S STATIONERY OFFICE
1954
PRICE 7*s* 6*d* NET

A Note on the Dynamic Stability of Aircraft at High-Subsonic Speeds when Considering Unsteady Flow

By

W. J. G. PINSKER

COMMUNICATED BY THE PRINCIPAL DIRECTOR OF SCIENTIFIC RESEARCH (AIR), MINISTRY OF SUPPLY

Reports and Memoranda No. 2904*

May, 1950

Summary.—The effect of an increase in speed relative to the speed of sound on the unsteady flow round a harmonically oscillating aerofoil, is to increase the lag of the aerodynamic forces and moments behind the deflection when the frequency is small. It is shown theoretically that this will result in a serious deterioration of the damping of both the lateral oscillation and the high frequency longitudinal oscillation with high Mach numbers. Use is made of derivatives calculated for flutter purposes to estimate the unsteady derivatives at aircraft oscillation frequencies. Illustrative examples are presented.

1. *Introduction.*—Calculations on the dynamic stability of aircraft are generally made with quasi-steady aerodynamic coefficients, *i.e.*, the forces and moments acting on each aerofoil surface at any instant of an oscillatory motion are calculated on the assumption that the aerofoil is in steady motion under the conditions pertaining at that instant.

In the past flight-test results have confirmed the quasi-steady theory within the accuracy possible in such tests. Recent flight tests with the *Meteor*, however, showed a marked divergence between the measured damping in yaw with rudder fixed and theoretical estimations based on quasi-steady aerodynamic derivatives ; this divergence increased with Mach number. The difference between theory and experiment is shown in Fig. 1, where the logarithmic decrement δ of the directional oscillation is plotted as obtained from flight tests; quasi-steady theory and unsteady theory. It is seen that the observed loss in damping with higher Mach numbers can satisfactorily be explained by the effects of unsteady flow.

Recent flight tests on a tailless aircraft at high speeds have also tended to throw doubt on the quasi-steady theory and some experiments in the free-flight tunnel at Langley Field by W. E. Cotter[2] seem to confirm the results of theory considering the effect of unsteady flow on the damping in pitch of tailless models even with incompressible flow.

The effect on the damping of aircraft of taking into account the unsteady flow conditions was first considered by Glauert[1]. In common with more recent publications[9, 10] this treatment dealt only with incompressible flow. Under these conditions the effect of allowing for unsteady flow does not appear to be large for aerofoils oscillating about a point forward of the quarter-chord, at any rate for the range of frequencies likely to occur in flight.

In this report an attempt has been made to take into account the unsteady conditions in compressible flow. The treatment is confined to conditions when no shock-waves are present, and it is assumed that compressibility effects on the derivatives obey the Glauert Law.

* R.A.E. Report Aero. 2378, received 7th December, 1950.

Owing to the inadequacy of the basic data needed for this work, the results presented in this report are far from being complete, and the conclusions are therefore somewhat tentative. There seems little doubt however that with increasing Mach number the reduction in damping due to the unsteady flow conditions become very much more marked, and there are important implications of the theory on the damping of tailless aircraft at high speed. The purpose of this report is mainly to draw attention to these extremely important trends, and to suggest the lines along which future theoretical and experimental work should proceed in order to investigate them further.

After the completion of the work presented in this report an American paper[9] on the instability of the oscillation of an aerofoil in incompressible flow has been received which arrives at conclusions very similar to those represented by the stability boundary for Mach number = 0 in Figs. 9 and 10 of this report.

2. *The Physical Basis of the Theory of Unsteady Flow.*—For detailed information on the subject reference should be made to the extensive special literature, in particular to two recent publications by G. Temple[3] and A. I. Necrasov[4]. For readers who are not familiar with the aerodynamic theory of unsteady flow this section is intended to give a very brief description of the main physical phenomena involved. Generally the flow pattern and thus the pressure distribution round an aerofoil moving in a frictionless fluid is determined by the geometry of the aerofoil itself and by velocities induced by the free vortices, mainly those in the vortex wake behind the trailing edge of the aerofoil. In steady motion there is only one starting vortex which is assumed to be curled up at an infinite distance aft of the trailing edge.

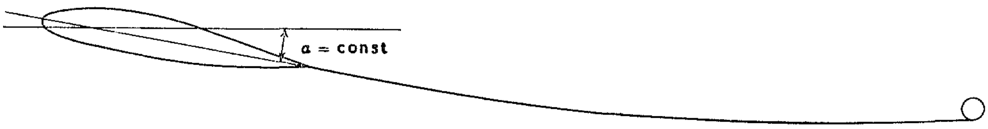

Vortex sheet and starting vortex aft of an aerofoil in steady motion after a sufficiently long time.

Since during an unsteady motion of an aerofoil the circulation round the aerofoil changes with time there is a continuous emission of new starting vortices into the wake, the distance of each vortex from the aerofoil increasing continuously with time as the aerofoil moves ahead. For example during an angular oscillation of an aerofoil the distribution of the free vortices aft of the wing will appear as sketched below.

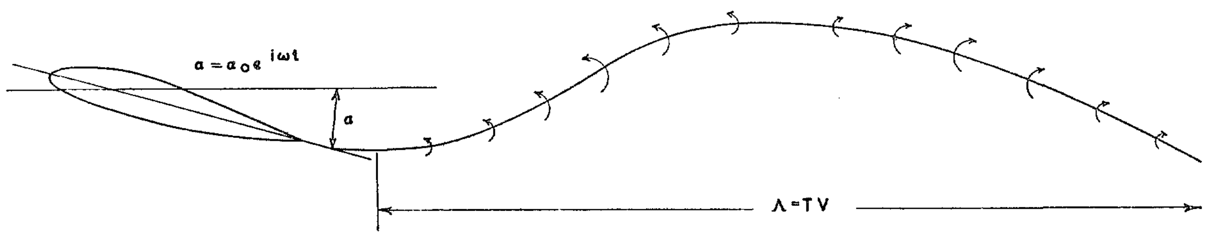

Free vortices in the wake of an aerofoil oscillating with the period T and the amplitude α_0.

Since the flow pattern round the aerofoil is affected by the contributions of the free vortices aft of the wing it must be expected that:

(*a*) the pressure distribution round an aerofoil in unsteady motion differs from that obtained with quasi-steady flow

(*b*) the main parameter describing the aerodynamic situation round a harmonically oscillating aerofoil will be the ratio between the chord c of the aerofoil and the wavelength $\Lambda = TV$ of the oscillation. This parameter is usually given as the reduced frequency

$$\lambda = \frac{2\pi c}{TV} . \qquad \qquad (1)$$

Matters become more complicated if wings with finite span are considered since then the induced flows from the unsteady trailing vortices have to be considered as well.

Another contribution to the forces acting upon a wing in unsteady motion which is not taken into account in the quasi-steady theory is caused by the reaction of the air being accelerated. This can be interpreted as an increase of the apparent mass and inertia of the aerofoil.

Finally the speed of sound enters into the calculations, since all disturbances and inductions can only be propagated with the speed of sound. Thus the velocity of propagation upstream relative to the aerofoil decreases with increasing Mach number and this will result in a delay of the aerodynamic forces at the aerofoil. The occurrence of shock-waves interferes with this simple physical concept. The calculations referred to in the next paragraphs only hold for compressible flow without shock-waves at the aerofoil concerned.

3. *Available Numerical Results.*—Numerical solutions for unsteady aerodynamic coefficients have been obtained by many authors. The most comprehensive results[5] available are for two-dimensional flow and they cover a wide range of speeds including incompressible flow conditions, the high-subsonic and the supersonic range of speeds. Solutions exist too for the unsteady coefficients due to flap deflections with various configurations[5,6]. Some authors[7,8] have investigated wings with finite aspect ratio up to the extreme case of an ocsillating circular wing[7]; but these solutions are for incompressible flow only.

As far as is known there are no reliable solutions for bodies of revolution representing fuselages or nacelles.

Another important limitation is that the majority of the theoretical solutions apply to constant-amplitude oscillations and they are therefore applicable strictly only to the boundary conditions of oscillations where the damping is exactly zero. Jones has shown how the unsteady forces vary with the damping of the supposed motion. In order, however, to simplify the approach in this paper, it will be assumed that the more extensive data on the derivatives applying to constant-amplitude oscillations, also apply to damped motions. It must be remembered, therefore, that the solutions given in this paper are strictly true only at the stability boundaries.

In papers dealing with the flutter problem, the aerodynamic coefficients are given in the form of complex numbers, *e.g.*,

$$l_\alpha = l_{\alpha R} + l_{\alpha i} \qquad (2)$$

where l_α is the rate of change of lift with angle α during an oscillation. The real part, $l_{\alpha R}$, is the component in phase with the deflection considered, the imaginary part is the component in phase with the corresponding rate of deflection, thus representing a damping or undamping effect. The apparent mass effect is sometimes given as a separate term which as a real number can be included in the real part of the coefficient, that is in phase with the deflection, though strictly only as long as the oscillation is of constant amplitude. This term is however small at the low frequencies to be considered and the error in including the acceleration term in the deflection term is small for the general, damped motion to be considered; the relationship between the two terms is of course dependent on frequency but since both are already functions of frequency no complication is added by putting them together. An example of the physical meaning of a complex coefficient is demonstrated in the figure, in which l_α defined according to equation (2) is plotted in the complex plane. The angle between the lift vector l_α and the deflection referred to α is the phase lag of the lift due to unsteady flow

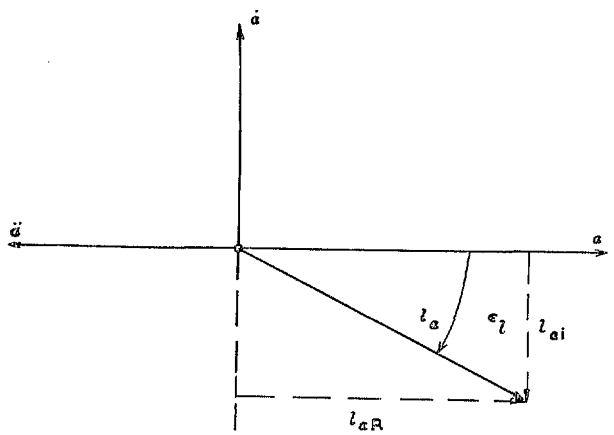

Physical interpretation of a complex lift coefficient in vector form.

$$\varepsilon_l = \omega t_l \qquad (3)$$

where ε_l is the phase-angle lag,

t_l is the lag in time.

The modes of oscillation generally considered in the compilation of flutter coefficients are an angular oscillation $\alpha_0 e^{i\omega t}$ and a translational oscillation $z_0 e^{i\omega t}$ of a rigid aerofoil; several modes of structural deformation are also considered, but we will not concern ourselves with them here, though strictly they should be considered when the frequency of the aircraft oscillation is approaching the frequencies of the wing modes, etc.

The axis of reference for the moments and for the centre of angular oscillation concerned, in the various papers is by no means constant. The figures extracted and presented in this report, however, have been corrected to refer uniformly to the quarter-chord point of the aerofoil considered. Most of the data has been extracted from the summary paper, Ref. 5; in this paper the coefficients have been presented in the form

$$l_z = (l_z + i\lambda l_{\dot{z}} + \lambda^2 l_{\ddot{z}}) \frac{\bar{z}}{c}, \text{ etc.} \qquad (4)$$

where Z is the lift force on the aerofoil

$\bar{z}$ is the oscillatory vertical deflection, etc.

They have all been converted to the form given above

$$l_z = l_{zR} + il_{zi}$$

with the acceleration term $l_{\ddot{z}}$ included in the l_{zR} term as explained above.

To give a few typical examples in the vector form, results are presented in Figs. 2 to 6 of calculations of the aerodynamic forces and moments of an oscillating wing with infinite aspect ratio in compressible subsonic flow extracted from Refs. 5 and 6. The coefficients are plotted as vector loci with Mach number and the reduced frequency λ as parameters. Fig. 2 shows the lift coefficient l_z, corresponding to a translatory oscillation; Fig. 3 the lift coefficient l_α due to an angular oscillation about the quarter-chord axis. The corresponding moment derivatives m_z and m_α are given in Figs. 4 and 5. Finally the unsteady flap effectiveness l_η for the oscillation of a flap with 20 per cent chord about its hinge axis is plotted in Fig. 6.

The vector loci of the lift coefficients l_α and l_η start with frequency zero ($\lambda = 0$) at a finite real value which corresponds to the steady lift slope a_1 (or control effectiveness a_2 respectively). With increasing frequency these lift forces are reduced in magnitude and delayed. At frequencies far beyond the range corresponding to the aircraft oscillations considered ($\lambda < \sim 0{\cdot}1$) a damping effect becomes more marked until at frequencies corresponding to $\lambda > \sim 0{\cdot}4$ the lift vectors cross the real axis and advance against the corresponding deflections.

With a translatory oscillation of an aerofoil the aerodynamic incidence is actually produced in the velocity phase $\dot{z}$ of the motion. Thus, when discussing l_z in Fig. 2, the corresponding quasi-steady term is a vector at the positive imaginary axis which increases in proportion to the frequency parameter λ. Compared with these quasi-steady values, the unsteady lift l_z behaves similarly to l_α and l_η.

4. *Equations of Motion.*—The assumptions made in developing the equations of motion to take into account the unsteady flow conditions are :—

(*a*) The oscillation will be assumed to be in two degrees of freedom, *i.e.*, the effect of variation in forward speed will be neglected in the longitudinal oscillation, and the rolling motion will be neglected in the directional oscillation.

(*b*) As explained in section 3, the derivatives obtained from constant-amplitude calculations will be assumed to be applicable to damped motions and the apparent mass effect of the air will be included in the derivatives in phase with deflection.

(*c*) The unsteady derivatives are all dependent in some way on the frequency parameter, λ, but in general the equations of motion will be derived assuming constant derivatives. If necessary the solution can be improved by successive approximation using the obtained frequency for an improved estimation of the derivatives.

When steady-flow conditions are being assumed the wing incidence $\alpha (= w/v)$ and the rate of pitch q are convenient variables to define the aerodynamic condition of the aircraft at any instant of the longitudinal oscillation. Similarly $\beta (= v/V)$ and rate of yaw r are convenient variables to define the directional motion.

With unsteady flow, however, the aerodynamic load exerted upon an aircraft with a given instantaneous incidence α differs according as to whether this incidence is produced by a change in attitude or by a translatory motion of the aircraft.

This means that a great number of terms has to be used for describing the aerodynamic loads on the aircraft when unsteady effects have to be taken into account. To avoid confusion with flutter theory we shall use the flutter parameters α^* and z and their derivatives. α^* is the angular deflection of the aerofoil during an oscillation and is identical with the parameter θ usual in aerodynamic theory for longitudinal motion, or ψ for directional motion. Similarly z defines the translatory motion so that for longitudinal motion

$$\dot{z} = -\gamma V \quad \ldots \quad (5)$$

and for directional motion

$$\dot{z} = -\dot{y} = -\chi V \quad \ldots \quad (6)$$

4.1. *Longitudinal Oscillation.*—The two independent variables describing the longitudinal oscillation are θ and γ as shown below.

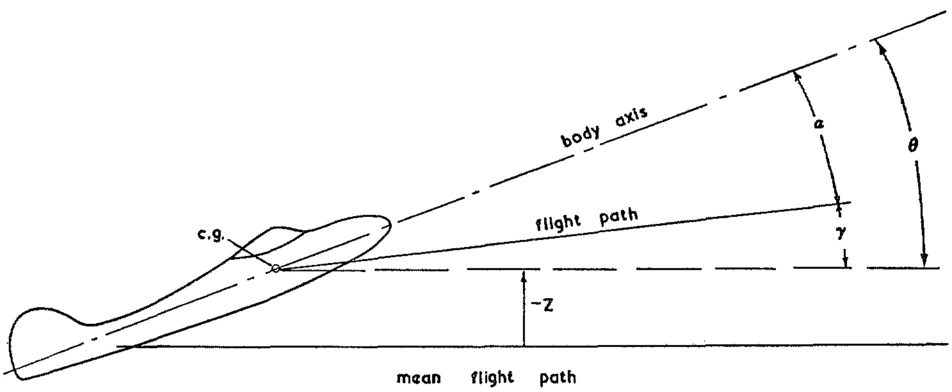

The downwash delay term $\bar{m}_{\dot{w}}$ will be assumed to maintain its quasi-steady definition since it is unlikely that unsteady values for the downwash ε are available. In order to express the required variable $\dot{\alpha}$ in terms of the above variables, use is made of the relationship

$$\alpha = \theta - \gamma \quad \ldots \quad (7)$$

Now the differential equations of the pitching moments M and the lift forces L can be written as :—

$$\left.\begin{aligned} &\frac{\partial M}{\partial \theta}\theta + \frac{\partial M}{\partial \gamma}\gamma + \frac{\partial M}{\partial(\dot{\theta}l/V)}\frac{l}{V}\dot{\theta} + \frac{\partial M}{\partial(\dot{\gamma}l/V)}\frac{l}{V}\dot{\gamma} + \frac{\partial M}{\partial(\dot{\alpha}l/V)}\frac{l}{V}(\dot{\theta} - \dot{\gamma}) = B\ddot{\theta} \\ &\frac{\partial L}{\partial \theta}\theta + \frac{\partial L}{\partial \gamma}\gamma + \frac{\partial L}{\partial(\dot{\theta}l/V)}\frac{l}{V}\dot{\theta} + \frac{\partial L}{\partial(\dot{\gamma}l/V)}\frac{l}{V}\dot{\gamma} = -m\ddot{z} = mV\dot{\gamma} \end{aligned}\right\} \quad \ldots \quad (8)$$

Expressing the aerodynamic derivatives in the usual way (*see* list of symbols and section 5) and introducing, as usual

$$\mu_1 = \frac{m}{\rho S l}, \quad \hat{t} = \frac{m}{\rho V S} \quad \text{and} \quad i_B = \frac{B}{m l^2}$$

this gives the determinant

$$\begin{vmatrix} \mu_1 \frac{m_\theta}{i_B} + \lambda\left(\frac{m_{\dot\theta}}{i_B} + \frac{\overline{m}_{\dot w}}{i_B}\right) - \lambda^2 & \mu_1 \frac{m_\gamma}{i_B} + \lambda\left(\frac{m_{\dot\gamma}}{i_B} - \frac{\overline{m}_{\dot w}}{i_B}\right) \\ z_\theta + \mu_1^{-1} z_{\dot\theta}\, \lambda & z_\gamma + \lambda\left(1 + \frac{z_{\dot\gamma}}{\mu_1}\right) \end{vmatrix} . \quad (9)$$

The corresponding frequency equation is a cubic

$$\lambda^3 + A_\alpha \lambda^2 + B_\alpha \lambda + C_\alpha = 0 \quad (10)$$

with the coefficients:

$$\left.\begin{aligned} A_\alpha &= -\left\{\frac{m_{\dot\theta}}{i_B} + \frac{\overline{m}_{\dot w}}{i_B} - \left(1 + \frac{z_{\dot\gamma}}{\mu_1}\right)^{-1}\left(z_\gamma + \frac{z_{\dot\theta}}{\mu_1}\left[\frac{m_{\dot\gamma}}{i_B} - \frac{\overline{m}_{\dot w}}{i_B}\right]\right)\right\} \\ B_\alpha &= -\left\{\mu_1 \frac{m_\theta}{i_B} - \left(1 + \frac{z_{\dot\gamma}}{\mu_1}\right)^{-1}\left(z_\theta\left[\frac{m_{\dot\gamma}}{i_B} - \frac{\overline{m}_{\dot w}}{i_B}\right] + z_{\dot\theta}\frac{m_\gamma}{i_B} - z_\gamma\left[\frac{m_{\dot\theta}}{i_B} + \frac{\overline{m}_{\dot w}}{i_B}\right]\right)\right\} \\ C_\alpha &= \mu_1\left(1 + \frac{z_{\dot\gamma}}{\mu_1}\right)^{-1}\left\{\frac{m_\gamma}{i_B} z_\theta - \frac{m_\theta}{i_B} z_\gamma\right\} \end{aligned}\right\} . \quad (11)$$

Contrary to the corresponding solution of the orthodox treatment with quasi-steady coefficients (equation (16)) the solution of equation (10) contains an aperiodic mode of motion the damping of which is described by the real root of approximately $\lambda_1 \simeq C_\alpha/B_\alpha$. The existence of such a non-periodic motion contradicts the definitions of the derivatives used which have been derived from an oscillatory type of motion. Thus the aperiodic solution λ_1 can be expected to have no physical reality. In fact the two terms in C_α (equation (11)) when considering steady motion are identical with the quasi-steady coefficients.

$$\left|\frac{m_\gamma}{i_B} z_\theta\right|_{\omega=0} \equiv \left|\frac{m_\theta}{i_B} z_\gamma\right|_{\omega=0} \equiv -\frac{m_w}{i_B} z_w . \quad (12)$$

Thus $C_\alpha = 0$ and consequently $\lambda_1 = 0$. The identity (12) holds with very good approximation for unsteady flow as well, *i.e.*,

$$\frac{m_\gamma}{i_B} z_\theta \simeq \frac{m_\theta}{i_B} z_\gamma .$$

Thus generally $C_\alpha \simeq 0$ and the cubic collapses into a quadratic

$$\lambda^2 + A_\alpha \lambda + B_\alpha = 0 \quad (13)$$

with the coefficients A_α and B_α from equations (11). Damping time t_α and period T_α of the high frequency longitudinal oscillation are then given by:

$$t_\alpha = \frac{2\hat{t}}{A_\alpha} \quad (14)$$

$$T_\alpha = \frac{2\pi\hat{t}}{\sqrt{(+B_\alpha - A_\alpha^2/4)}} \quad (15)$$

where $\hat{t} = \frac{m}{\rho S V}$.

When comparing equations (11) with the orthodox solution with quasi-steady derivatives:

$$\left.\begin{aligned} A_\alpha{}^* &= -\left\{\frac{m_q}{i_B} + z_w + \frac{\overline{m}_{\dot{w}}}{i_B}\left(1+\frac{z_q}{\mu_1}\right)\right\} \\ B_\alpha{}^* &= -\left\{\mu_1\frac{m_w}{i_B}\left(1+\frac{z_q}{\mu_1}\right) - \frac{m_q}{i_B}z_w\right\}\end{aligned}\right\} \quad \ldots \quad \ldots \quad \ldots \quad (16)$$

it is seen that apart from minor contributions the following coefficients are comparable with respect to their effect on damping and frequency of the longitudinal oscillation

$$\text{quasi-steady flow}\left\{\begin{matrix} m_w & \text{corresponds to} & m_\theta \\ m_q & ,, \quad ,, & m_{\dot\theta} \\ z_w & ,, \quad ,, & -z_\gamma \\ m_{\dot w} & ,, \quad ,, & m_{\dot w}\end{matrix}\right\}\text{unsteady flow.}$$

Therefore it can be concluded that an approximated estimation of the effect of unsteady flow on the longitudinal oscillation can be obtained by substituting the above unsteady terms for the corresponding quasi-steady derivatives. This process may be advantageous when converting existing quasi-steady solutions of more complicated degree into unsteady solutions, in particular the lateral stability case with freedom in roll, and also for treatments of control free stability.

4.2. *Directional Oscillation.*—The two parameters defining motion with two degrees of freedom are yawing ψ and the lateral displacement of the c.g. : y. As shown in equation (16) and the figure below, y can be expressed by the azimuth angle at the flight path χ.

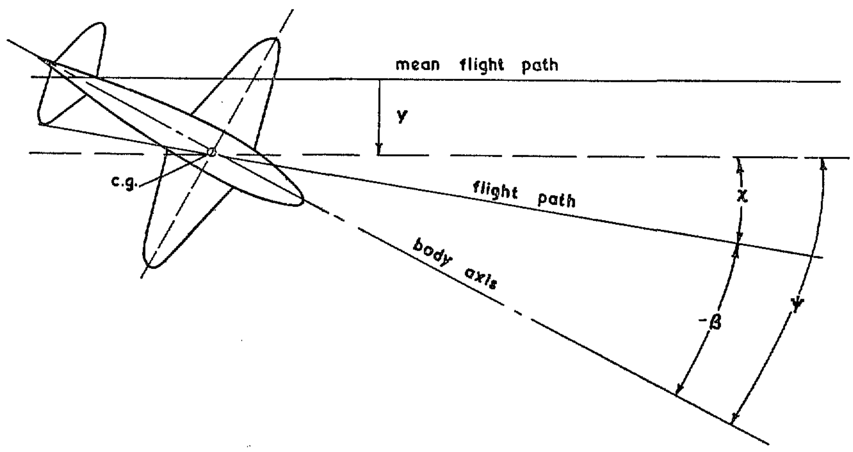

Sidewash can be neglected. Then the differential equations of the yawing moments N and the side forces Y for unsteady aerodynamic derivatives can be written:

$$\frac{\partial N}{\partial \psi}\psi + \frac{\partial N}{\partial \chi}\chi + \frac{\partial N}{\partial(\dot\psi b/2V)}\frac{b}{2V}\dot\psi + \frac{\partial N}{\partial(\dot\chi b/2V)}\frac{b}{2V}\dot\chi = C\ddot\psi \quad \ldots \quad \ldots \quad (17)$$

$$\frac{\partial Y}{\partial \psi}\psi + \frac{\partial Y}{\partial \chi}\chi + \frac{\partial Y}{\partial(\dot\psi b/2V)}\dot\psi\frac{b}{2V} + \frac{\partial Y}{\partial(\dot\chi b/2V)}\frac{b}{2V}\dot\chi = m\ddot y = mV\dot\chi \,. \quad (18)$$

Introducing as usual $\hat{t}$, $\mu_2 = 2m/\rho Sb$ and $i_c = 4C/mb^2$ and performing the same operation as with the longitudinal stability equations one obtains a cubic

$$\lambda^3 + A_\psi\lambda^2 + B_\psi\lambda + C_\psi = 0 \quad \ldots \quad \ldots \quad \ldots \quad \ldots \quad (19)$$

with the coefficients:

$$\left.\begin{aligned} A_\psi &= -\left\{\frac{n_{\dot\psi}}{i_c} + \left(1 - \frac{y_{\dot\chi}}{\mu_2}\right)^{-1}\left(\frac{n_{\dot\chi}\,y_\chi}{i_c\,\mu_2} + y_\chi\right)\right\} \\ B_\psi &= -\left\{\mu_2\frac{n_\psi}{i_c} + \left(1 - \frac{y_{\dot\chi}}{\mu_2}\right)^{-1}\left(\frac{n_\chi}{i_c}y_{\dot\psi} + \frac{n_{\dot\chi}}{i_c}y_\psi - \frac{n_{\dot\psi}}{i_c}y_\chi\right)\right\} \\ C_\psi &= -\mu_2\left(1 - \frac{y_{\dot\chi}}{\mu_2}\right)^{-1}\left(\frac{n_\chi}{i_c}y_\psi - \frac{n_\psi}{i_c}y_\chi\right) \end{aligned}\right\} \quad \ldots \quad \ldots \quad (20)$$

Again the identity

$$\left|\frac{n_\chi}{i_c}y_\psi\right|_{\omega=0} \equiv \left|\frac{n_\psi}{i_c}y_\chi\right|_{\omega=0} \equiv \frac{n_v}{i_c}y_v \quad \ldots \quad (21)$$

makes $C_\psi = 0$ and reduces the frequency equation to a quadratic with the coefficients A_ψ and B_ψ from equation (20). Damping time t_ψ and period T_ψ of the directional oscillation are then

$$t_\psi = \frac{2\hat{t}}{A_\psi} \quad \ldots \quad (22)$$

$$T_\psi = \frac{2\pi\hat{t}}{\sqrt{(+B_\psi - A_\psi^2/4)}}\,. \quad \ldots \quad (23)$$

The coefficients of the corresponding quasi-steady frequency equation read

$$\left.\begin{aligned} A_\psi^* &= -\left\{\frac{n_r}{i_c} + y_v\right\} \\ B_\psi^* &= +\left\{\mu_2\frac{n_v}{i_c}\left(1 - \frac{y_r}{\mu_2}\right) + \frac{n_r}{i_c}y_v\right\} \end{aligned}\right\} \quad \ldots \quad (24)$$

Comparison between equations (20) and (24) again indicates that there are main terms which can be substituted with an approximated treatment:

$$\text{quasi-steady flow}\left\{\begin{array}{llll} n_v & \text{corresponds to} & - & n_\psi \\ n_r & ,, & ,, & n_{\dot\psi} \\ y_v & ,, & ,, & y_\chi \end{array}\right\}\text{unsteady flow.}$$

5. *The Formation of the Aerodynamic Derivatives for the Complete Aircraft.*—Having obtained the solution of the equations for longitudinal and directional oscillations in section 4, all that remains to do is to substitute the values of the unsteady aerodynamic derivatives into the expressions for frequency and damping. A brief explanation is given in this section of the method used to obtain the particular derivatives for an aircraft from the general flutter derivatives.

Now as explained in section 3, the flutter derivatives used in this report are given in the form

$$l_\alpha = l_{\alpha R} + i l_{\alpha i}\,, \text{ etc.}$$

where

$$\left.\begin{aligned} l_{\alpha R} &= \frac{\partial C_{LR}}{\partial\alpha^*} = f\left(\lambda = \frac{\omega c}{V}\,, \text{Mach number}, A\right) \\ l_{\alpha i} &= \frac{\partial C_{Li}}{\partial\alpha^*} = f\left(y, \text{Mach number}, A\right) \end{aligned}\right\} \quad \ldots \quad (25)$$

and α^* is the angular deflection of an aerofoil during an angular oscillation. Correspondingly the lift due to a translatory oscillation of an aerofoil is given by

$$l_{zR} = \frac{\partial C_{LR}}{\partial(z/c)} \quad \text{and} \quad l_{zi} = \frac{\partial C_{Li}}{\partial(z/c)}\,. \quad \ldots \quad (26)$$

The moment coefficients $C_{\overline{M}}$ about the axis of reference of an individual aerofoil (in this report the quarter-chord line is used throughout) are represented analogously by complex numbers:—

$$m_{\alpha R} = \frac{\partial C_{\overline{M}R}}{\partial \alpha^*} \qquad m_{\alpha i} = \frac{\partial C_{\overline{M}i}}{\partial \alpha^*} \quad \ldots \quad (27)$$

$$m_{zR} = \frac{\partial C_{\overline{M}R}}{\partial (z/c)} \qquad m_{zi} = \frac{\partial C_{\overline{M}i}}{\partial (z/c)} . \quad \ldots \quad (28)$$

All these coefficients are functions of λ, Mach number and aspect ratio A. Numerical figures for the flutter coefficients in the form needed for the estimation of the stability derivatives are given in Tables 1 and 2. These values are computed from Ref. 5 and hold for two-dimensional flow with a thin aerofoil. If a_1 is the lift slope of the actual aerofoil with an aspect ratio A then we can obtain an approximated estimation of the three-dimensional value by multiplying the thin-aerofoil flutter derivative by a factor $a_1/2\pi$. This value of a_1 can either be taken from steady wind-tunnel tests or it is approximately given by the relation

$$a_1 = \frac{A}{A+2} a_0 . \quad \ldots \quad (29)$$

5.1. *Longitudinal Derivatives.*—We have to evaluate the terms:

$$z_\theta,\ z_{\dot\theta},\ z_y,\ z_{\dot y}$$

$$m_\theta,\ m_{\dot\theta},\ m_y,\ m_{\dot y},\ \overline{m}_{\dot w} .$$

Dealing with the θ and $\dot\theta$ terms first and remembering that the flutter α^* is identical with the θ used in the stability equations, consider the general case of any aerofoil (wing or tailplane) hinged at a point l_A forward of the quarter-chord point.

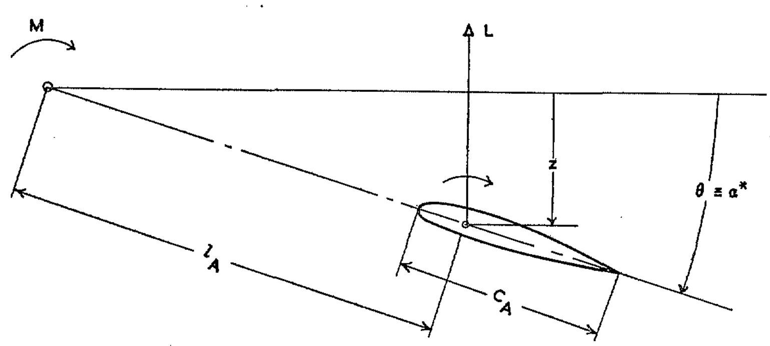

Then the total lift in terms of the derivatives given for the quarter-chord point is

$$L = \tfrac{1}{2}\rho V^2 S_A \left(l_{\alpha R}\theta + i l_{\alpha i}\theta + l_{zR}\theta \frac{l_A}{c_A} + i l_{zi}\theta \frac{l_A}{c_A}\right) \ldots \quad (30)$$

Now remembering that we are evaluating the derivatives for undamped oscillations only we have

$$\dot\theta = i\omega\theta \quad \ldots \quad (31)$$

and this can be used to transform equation (30) into

$$L = \tfrac{1}{2}\rho V^2 S_A \left(l_{\alpha R}\theta + i l_{\alpha i}\frac{\dot\theta}{i\omega} + l_{zR}\theta \frac{l_A}{c_A} + i l_{zi}\frac{\dot\theta}{i\omega}\frac{l_A}{c_A}\right) . \quad \ldots \quad (32)$$

This equation contains real terms only and can be split up into the partial derivatives

$$z_\theta = -\tfrac{1}{2}\frac{\partial C_L}{\partial \theta} = -\tfrac{1}{2}\frac{S_A}{S}\left\{l_{\alpha R} + \frac{l_A}{c_A} l_{zR}\right\} \quad \ldots \quad (33)$$

and

$$z_\theta = -\tfrac{1}{2}\frac{\partial C_L}{\partial(\theta l/V)} = -\tfrac{1}{2}\frac{S_A}{S}\left\{l_{\alpha i}\frac{V}{l\omega} + l_{zi}\frac{l_A}{c_A}\frac{V}{\omega l}\right\}. \quad \ldots \quad (34)$$

Substituting $\lambda = \omega c_A/V$ this gives

$$z_\theta = -\tfrac{1}{2}\frac{S_A}{S}\left\{\frac{c_A}{l}\frac{l_{\alpha i}}{\lambda} + \frac{l_A}{c_A}\frac{l_{zi}}{\lambda}\right\}. \quad \ldots \quad (35)$$

Examination of the derivative data, however, shows that $l_{\alpha i}$ and l_{zi} vary approximately linearly with λ over the range $0 < \lambda < \sim 0\cdot08$ which is roughly the range to be considered in dynamic stability problems. The equation (35) can therefore be rewritten in the form

$$z_\theta = -\tfrac{1}{2}\frac{S_A}{S}\frac{c_A}{l}\left\{\frac{\partial l_{\alpha i}}{\partial\lambda} + \frac{l_A}{c_A}\frac{\partial l_{zi}}{\partial\lambda}\right\}. \quad \ldots \quad (36)$$

The moment M about the c.g. of an aircraft as produced by an aerofoil oscillating at an arm l_A from the c.g. is given by

$$M = M_0 - Ll_A. \quad \ldots \quad (37)$$

Adding these two contributions the moment derivatives with respect to θ and $\dot\theta$ are obtained:

$$m_\theta = \frac{c}{2l}\frac{\partial C_M}{\partial\theta} = \tfrac{1}{2}\frac{S_A}{S}\frac{c_A}{l}\left\{m_{\alpha R} + (m_{zR} - l_{\alpha R})\frac{l_A}{c_A} - l_{zR}\left(\frac{l_A}{c_A}\right)^2\right\} \quad \ldots \quad (38)$$

$$m_{\dot\theta} = \frac{c}{2l}\frac{\partial C_M}{\partial(\dot\theta l/V)} = \tfrac{1}{2}\frac{S_A}{S}\left(\frac{c_A}{l}\right)^2\left\{\frac{\partial m_{\alpha i}}{\partial\lambda} + \left(\frac{\partial m_{zi}}{\partial\lambda} - \frac{\partial l_{\alpha i}}{\partial\lambda}\right)\frac{l_A}{c_A} - \frac{\partial l_{zi}}{\partial\lambda}\left(\frac{l_A}{c_A}\right)^2\right\}. \quad \ldots \quad (39)$$

For the determination of the stability derivatives with respect to γ and $\dot\gamma$ the kinematic relationship between $\dot z$ and γ (equation (5)) must be remembered. Further corresponding to equation (31):

$$z = \frac{\dot z}{i\omega}; \qquad \gamma = \frac{\dot\gamma}{i\omega}; \qquad z = -\frac{\gamma V}{i\omega}. \quad \ldots \quad (40)$$

The total lift L acting on an aerofoil A during translatory oscillation of the c.g. of the aircraft is given by:

$$L = \tfrac{1}{2}\rho V^2 S_A\left\{{}_z l_R\frac{z}{c_A} + il_{zi}\frac{z}{c_A}\right\}. \quad \ldots \quad (41)$$

Using equation (40) this can be transformed into an equation having real components only:

$$L = -\tfrac{1}{2}\rho V^2 S_A\left\{-l_{zR}\frac{V}{c_A}\frac{\dot\gamma}{\omega^2} + il_{zi}\frac{V}{c_A}\frac{\gamma}{i\omega}\right\}. \quad \ldots \quad (42)$$

This gives the partial derivatives required:

$$z_\gamma = -\tfrac{1}{2}\frac{\partial C_L}{\partial\gamma} = \tfrac{1}{2}\frac{S_A}{S}\frac{\partial l_{zi}}{\partial\lambda} \quad \ldots \quad (43)$$

$$z_{\dot\gamma} = -\tfrac{1}{2}\frac{\partial C_L}{\partial(\dot\gamma l/V)} = -\tfrac{1}{2}\frac{S_A}{S}\frac{c_A}{l}\frac{l_{zR}}{\lambda^2}. \quad \ldots \quad (44)$$

As seen from Table II l_{zR} (and m_{zR} as used later for $m_{\dot\gamma}$ in equation (47)) is small and changes approximately with λ^2—mainly because it represents as a major contribution the apparent mass of the air. Thus it is felt that the use of a constant derivative for $\partial l_{zR}/\partial\lambda^2$ and later $\partial m_{zR}/\partial\lambda^2$ does not involve any appreciable inaccuracies and the equation (44) can be rewritten:

$$z_{\dot\gamma} = -\frac{1}{2}\frac{S_A}{S}\frac{c_A}{l}\frac{\partial l_{zR}}{\partial\lambda^2} . \qquad (45)$$

For the determination of the corresponding moment derivatives equation (37) has to be applied which gives finally:

$$m_\gamma = \frac{c}{2l}\frac{\partial C_M}{\partial\gamma} = \frac{1}{2}\frac{S_A}{S}\frac{c_A}{l}\left\{\frac{\partial l_{zi}}{\partial\lambda}\frac{l_A}{c_A} - \frac{\partial m_{zi}}{\partial\lambda}\right\} \qquad (46)$$

$$m_{\dot\gamma} = \frac{c}{2l}\frac{\partial C_M}{\partial(\dot\gamma l/V)} = \frac{1}{2}\frac{S_A}{S}\left(\frac{c_A}{l}\right)^2\left\{\frac{\partial m_{zR}}{\partial\lambda^2} - \frac{\partial l_{zR}}{\partial\lambda^2}\frac{l_A}{c_A}\right\} . \qquad (47)$$

If the equations (33 to 47) are applied for the evaluation of the contributions of wing$_W$ and tailplane$_T$ the geometric parameters S_A, l_A, c_A in these expressions have to be substituted by the corresponding values of the wing (S, l_W, c) or tailplane (S_T, l, c_T) respectively.

In dealing with the effect of downwash on the tail we will as usual divide the total effect into two components:

(*a*) First, assuming that the magnitude of downwash at the tail corresponds to that which would be developed in a steady state with the angle of wing incidence at the same value as that at the instant considered.

(*b*) Then allowing for the lag in downwash produced

(i) by the lagging of the wing lift behind the wing incidence due to unsteady flow

(ii) by the time delay in the flow reaching the tail from the wing.

This part constitutes the $m_{\dot w}$ term.

The first effect of the downwash reducing the actual incidence of the tailplane can be provided for by multiplying all terms with the tailplane derivatives which can be associated with a simultaneous change of incidence at the wing with a factor

$$\left(1 - \frac{d\varepsilon}{d\alpha}\right) . \qquad (48)$$

These are the coefficients l_α and m_α in the derivatives with respect to θ and $\dot\theta$ and the whole expression for the tailplane contribution to the derivatives with respect to γ and $\dot\gamma$.

This need only be demonstrated by two examples:

$$(m_\theta)_T = \frac{1}{2}\frac{S_T}{S}\frac{c_T}{l}\left\{\left(1 - \frac{d\varepsilon}{d\alpha}\right)\left(m_{\alpha R} - l_{\alpha R}\frac{l}{c_T}\right) + m_{zR}\frac{l}{c_T} - l_{zR}\left(\frac{l}{c_T}\right)\right\} \qquad (49)$$

$$|m_{\dot\gamma}|_T = \frac{1}{2}\frac{S_T}{S}\left(\frac{c_T}{l}\right)^2\left(1 - \frac{d\varepsilon}{d\alpha}\right)\left\{\frac{\partial m_{zR}}{\partial\lambda^2} - \frac{\partial l_{zR}}{\partial\lambda^2}\frac{l}{c_T}\right\} . \qquad (50)$$

From the discussion of equations (11) and (16) and the comparability of the moment coefficients $m_w \simeq m_\theta$, $m_q \simeq m_{\dot\theta}$ it can be concluded that in the modes of oscillation present during the longitudinal motion considered θ and γ are of quite different order and γ obviously does not contribute much to the pitching moments, *i.e.*,

$$\theta \simeq \alpha ; \qquad \gamma \ll \theta .$$

Thus for the determination of the downwash delay, which is defined as a derivative with respect to $\dot{\alpha}$, only the lag of l_α against $\alpha^* \equiv \theta$ will be considered. The downwash, ε, arrives at the tailplane with a phase lag ε_t against θ which can be added to the above discussed two contributions

$$\varepsilon_t = \omega t_l = \omega \frac{l}{V} - \left| \frac{l_{\alpha i}}{l_{\alpha R}} \right|_{WING} . \qquad (51)$$

This can be used for determining the derivative

$$\overline{m}_{\dot{w}} = \frac{c}{2l} \frac{\partial C_M}{\partial(\dot{\alpha}l/V)} \simeq \tfrac{1}{2} \left(l_{\alpha R}\right)_T \frac{S_T}{S} \frac{d\varepsilon}{d\alpha} \left\{ 1 - \frac{c}{l} \left(\frac{\partial l_{\alpha i}/\partial \lambda}{l_{\alpha R}} \right)_W \right\} . \qquad (52)$$

5.2. *Directional Derivatives.*—The only aerofoil surface to be considered with lateral motion with two degrees of freedom is the fin. Remembering equation (6) and the conclusion from section 4 the following identities can be used for the determination of the derivatives:

$$\text{flutter terms} \left\{ \begin{array}{l} L \equiv Y \\ M \equiv N \\ z \equiv -y \\ \alpha^* \equiv \psi \end{array} \right\} \text{stability terms.} \qquad (53)$$

Sidewash can be neglected. Performing the same transformations as in section 5.1 the lateral stability derivatives are obtained.

$$y_\psi = \tfrac{1}{2} \frac{\partial C_y}{\partial \psi} = \tfrac{1}{2} \frac{S_F}{S} \left\{ l_{\alpha R} + \frac{l_F}{c_F} l_{zR} \right\} \qquad (54)$$

$$y_{\dot\psi} = \tfrac{1}{2} \frac{\partial C_y}{\partial(\dot\psi b/2V)} = \frac{S_F}{S} \frac{c_F}{b} \left\{ \frac{\partial l_{\alpha i}}{\partial \lambda} + \frac{\partial l_{zi}}{\partial \lambda} \frac{l_F}{c_F} \right\} \qquad (55)$$

$$n_\psi = \frac{\partial C_N}{\partial \psi} = \frac{S_F}{S} \frac{c_F}{b} \left\{ m_{\alpha R} + \frac{l_F}{c_F} (m_{zR} - l_{\alpha R}) - l_{zR} \left(\frac{l_F}{c_F} \right)^2 \right\} \qquad (56)$$

$$n_{\dot\psi} = \frac{\partial C_N}{\partial(\dot\psi b/2V)} = \frac{S_F}{S} \frac{2c_F}{b} \frac{l_F}{b} \left\{ \frac{\partial m_{\alpha i}}{\partial \lambda} \frac{c_F}{l_F} - \frac{\partial l_{\alpha i}}{\partial \lambda} + \frac{\partial m_{zi}}{\partial \lambda} - \frac{\partial l_{zi}}{\partial \lambda} \frac{l_F}{c_F} \right\} \qquad (57)$$

$$y_\chi = \tfrac{1}{2} \frac{\partial C_y}{\partial \chi} = -\tfrac{1}{2} \frac{S_F}{S} \frac{\partial l_{zi}}{\partial \lambda} \qquad (58)$$

$$y_{\dot\chi} = \tfrac{1}{2} \frac{\partial C_y}{\partial(\dot\chi b/2V)} = \frac{S_F}{S} \frac{c_F}{b} \frac{\partial l_{zR}}{\partial \lambda^2} \qquad (59)$$

$$n_\chi = \frac{\partial C_N}{\partial \chi} = \frac{S_F}{S} \frac{c_F}{b} \left\{ \frac{\partial l_{zi}}{\partial \lambda} \frac{l_F}{c_F} - \frac{\partial m_{zi}}{\partial \lambda} \right\} \qquad (60)$$

$$n_{\dot\chi} = \frac{\partial C_N}{\partial(\dot\chi b/2V)} = \frac{S_F}{S} \frac{2c_F}{b} \left\{ \frac{\partial m_{zR}}{\partial \lambda^2} \frac{c_F}{b} - \frac{\partial l_{zR}}{\partial \lambda^2} \frac{l_F}{b} \right\} . \qquad (61)$$

5.3. *Fuselage and Nacelles.*—If unsteady aerodynamic coefficients are known for bodies of revolution such as fuselages and nacelles, they can be expressed in the form of the above determined derivatives. At present no such solutions exist. Thus one is confined to the use of known quasi-steady values. These can best be expressed in terms of the above defined unsteady derivatives by using the following identities which hold for infinitely slow motion ($\omega \rightarrow 0$).

$$\left.\begin{array}{llll} z_\theta \equiv z_w & m_\theta \equiv m_w & y_\psi \equiv -y_v & n_\psi \equiv -n_v \\ z_{\dot\theta} \equiv z_q & m_{\dot\theta} \equiv m_q & y_{\dot\psi} \equiv y_r & n_{\dot\psi} \equiv n_r \\ z_\gamma \equiv -z_w & m_\gamma \equiv -m_w & y_\chi \equiv y_v & n_\chi \equiv n_v \\ \multicolumn{4}{c}{z_{\dot\gamma} = m_{\dot\gamma} = y_{\dot\chi} = n_{\dot\chi} = 0} \end{array}\right\} \quad (62)$$

6. *Numerical Examples.*—The consequences of unsteady flow on the dynamic stability of aircraft will best be illustrated by numerical examples. For these specific calculations two types of aircraft have been chosen which can be expected to respond differently to the particular effects of unsteady flow.

Example A is an orthodox tailed aircraft with a relatively long tail arm, which thus possesses basically sound damping both in pitch and in yaw.

Example B is the tailless version of A with a fin at a relatively short arm. When discussing lateral stability this example will therefore be referred to as short-tailed version as compared with the long-tailed version A. There are two versions of the tailless aircraft B considered with longitudinal stability. They are distinguished by different sizes of the fuselage.

Since there are no unsteady aerodynamic coefficients available for sweptback wings the wings in both cases are assumed to be identical both without sweep. It must be noted that for a wing with sweep the damping in pitch with unsteady flow is probably much higher than for a straight wing.

The geometrical data for both aircraft are given in Table 3. The unsteady aerodynamic derivatives have been obtained with the formulae derived in section 5. The two-dimensional lift slope, a_0, has been assumed as $5 \cdot 65$ for all aerofoils concerned; the finite aspect ratio of each surface has been allowed for by using equation (29). For the tailed aircraft A, the downwash slope, $d\varepsilon/d\alpha$, has been assumed to be $0 \cdot 3$. The fuselage contributions are dealt with as indicated in section 5.3. In all cases considered the calculations have been done for 4 different Mach numbers ($0, 0 \cdot 5, 0 \cdot 7, 0 \cdot 8$) and the results are presented in Tables 4 to 6.

Table 4 refers to the longitudinal stability of the tailed aircraft, A. First the unsteady aerodynamic derivatives are given as wing contributions (suffix $_W$) and tailplane contributions (suffix $_T$). The complete derivatives including fuselage contributions as well are given as sums ($\Sigma \ldots$). The coefficients of the frequency equation (equation (13)) are given in the dimensionless form A_α and B_α. The μ_1 and μ_2 used correspond to ground level.

The change of dynamic stability with altitude has been checked in all cases considered. Apart from the generally known decrease in damping proportional to ρ a slight change of the damping coefficient A_α (and A_α for directional stability) is to be expected since some of the terms contain μ_1 or μ_2 respectively. These terms, however, are so small that no appreciable change of the stability boundary has been observed.

For the determination of the reduced frequencies λ as the important parameters for the unsteady derivatives the indicated wavelength of the longitudinal oscillation is computed from equation (15) which gives

$$\Lambda_{\alpha i} = T_\alpha V_i = 22 \cdot 7 \sqrt{\left(\frac{\mu_1 Wl/S}{+ B_\alpha - A_\alpha^2/4}\right)} . \quad (63)$$

The corresponding expression for the wavelength of the directional oscillation is

$$\Lambda_{\psi i} = T_\psi V_i = 16 \cdot 07 \sqrt{\left(\frac{\mu_2 (W/S) b}{+ B_\psi - A_\psi^2/4}\right)} . \quad (64)$$

Since the reduced frequency is the ratio of the individual chord c to the wavelength Λ

$$\lambda = \frac{2\pi c}{\Lambda} \quad \ldots \quad (65)$$

the formulae (63) or (64) respectively can be used to evaluate the reduced frequency by considering the relationship between the indicated wavelength Λ_i and the true wavelength Λ

$$\lambda = 2\pi \frac{c}{\Lambda_i} \sqrt{\sigma} \quad \ldots \quad (66)$$

For the determination of the real parts of the flutter coefficients (Table II) needed, the value of λ for the various aerofoil surfaces has been first estimated by a quasi-steady approximation for the periods of the oscillations concerned. The values for the reduced frequencies λ given in Tables 4 to 7, however, have been obtained from the actual frequencies resulting from the calculations with unsteady derivatives.

The corresponding figures for the longitudinal oscillation of the tailless aircraft B are given in Table 5 for two different c.g. positions, *i.e.*, for the different values of the distance l_W of the quarter-chord of the wing from the c.g. of the aircraft. Table 6 contains the corresponding figures for tailless version with a smaller fuselage.

The corresponding figures for the directional stability calculations for both the long-tailed version (A) and the short-tailed version (B) are given in Table 7.

The most important results, the values of the damping roots A_α and A_ψ for longitudinal and directional oscillations respectively, are plotted against Mach number in Figs. 7 and 8. The results of the calculations with unsteady derivatives are represented by full lines. Corresponding calculations have been done with quasi-steady aerodynamic derivatives which are assumed to change with Mach number according to Glauert's rule. The results of these calculations are presented for comparison and shown by dotted lines.

As Fig. 7 shows, the results with unsteady derivatives compare very favourably with quasi-steady results for the damping of the longitudinal oscillations of the tailed aircraft. The close agreement seen, however, is mere coincidence. It results from adding basically different effects, namely damping in pitch m_θ and downwash delay $m_{\dot{w}}$. With appreciable downwash present, this tendency can generally be expected for conventionally tailed aircraft.

The damping of the longitudinal oscillation of the tailless aircraft (B) may, however, be radically altered when considering the effects of unsteady flow at high subsonic speeds. Much depends, with the simple theory used, on the value of l_W/c assumed, *i.e.*, the distance between the c.g. and the aerodynamic centre of the wing in terms of the mean chord. With well-forward c.gs. with a l_W/c of between 0·1 and 0·2 (such values correspond roughly with those of the DH.108), the destabilisation of the dynamic stability is very marked at high Mach numbers, neutral stability being predicted at Mach numbers between 0·7 and 0·85. With a l_W/c of 0·05, however the damping calculated at high Mach numbers using unsteady-flow theory is very similar to that obtained using quasi-steady flow ; this value of l_W/c could only be obtained on an aircraft with a very small or negligible fuselage, for the destabilising effect of the fuselage would otherwise cause an unacceptably low or a negative static margin. Thus this admittedly approximate theory of unsteady flow is predicting in some practical condition of aircraft layout, a negative damping of the longitudinal oscillation at Mach numbers where the theory does not necessarily break down due to the presence of shock-waves on the wing surface.

The results of the calculations of the damping of the directional oscillation of the two aircraft considered are shown in the diagram Fig. 8. It is seen that calculations with quasi-steady derivatives give far too optimistic results. In both examples considered a rapid deterioration of damping due to the effects of unsteady flow occurs at Mach numbers beyond 0·6 and an undamped oscillation would appear likely with the short-tailed aircraft at a Mach number just above 0·8.

The aircraft with the fin at the longer arm has the better basic damping, and the undamping effects of unsteady flow appear less severe; actual instability would not therefore be predicted until the assumptions on which the aerodynamic derivatives used in this paper depend break down due to the presence of shock-waves.

The main effects of unsteady flow on the aircraft oscillations are mainly represented in the damping derivatives $m_{\dot\theta}$ and $n_{\dot\psi}$ respectively. They are generally smaller as compared with the corresponding quasi-steady values of m_q and n_r respectively, and they will become undamping with higher Mach numbers in most cases. The other major damping terms affecting the aircraft oscillations considered, i.e., z_γ and y_χ for longitudinal and directional motion respectively, are hardly altered when considering the effects of unsteady flow. Thus dynamic stability of the aircraft oscillations is maintained up to Mach numbers above those associated with the change in sign of the damping derivatives $m_{\dot\theta}$ or $n_{\dot\psi}$ respectively.

7. *The Stability of an Oscillating Wind Vane.*—Another more simple way of demonstrating the effects of unsteady flow is by investigating the stability of the oscillation of a wind vane as it changes with the length of the arm of suspension and Mach number. This may also be interpreted as the stability of the longitudinal oscillation or directional oscillation in one degree of freedom. In this case the wind vane can be identified with the fin or tailplane (or wing for the longitudinal oscillation of a tailless aircraft) of the aircraft considered.

Dynamic stability of such a system is present if the imaginary part of the resultant moment exerted upon the hinge during the oscillation is positive, *i.e.*, there is a component of the moment opposing the motion of the vane. If $m_{\alpha i\,0}$ is the imaginary part of the hinge moment then this condition reads

$$m_{\alpha i\,0} = \frac{\partial C_{M\,0}}{\partial \alpha^*} > 0 \,. \qquad \ldots \quad (67)$$

Using the flutter derivatives as before and remembering that the translatory deflection of the quarter-chord of the aerofoil surface of the wind vane of an arm l from the hinge axis is $z = \alpha^* l$, $m_{\alpha i\,0}$ is given as

$$m_{\alpha i\,0} = m_{\alpha i} + m_{zi}\frac{l}{c} - l_{\alpha i}\frac{l}{c} - l_{zi}\left(\frac{l}{c}\right)^2 . \qquad \ldots \quad (68)$$

The flutter derivatives are functions of Mach number and λ, thus the stability boundary will also depend on Mach number, λ and the relative arm, l/c, of the vane. The results of calculations for two-dimensional unsteady flow corresponding to the figures given in Tables 1 and 2 are plotted as stability boundaries in the $l/c-\lambda$ plane with Mach number as a parameter, in Fig. 9. It is seen that even with incompressible flow an unstable region exists for the range of hinge axes between the quarter-chord point and $0{\cdot}7c$ ahead of the quarter-chord with relatively small reduced frequencies. When suspended aft of the quarter-chord the wind vane is damped, but of course—without any additional spring in the system—statically unstable. With increasing Mach number the unstable region extends towards longer arms l and higher frequencies λ. A cross-plotting of the stability diagram against Mach number with the arm l/c as parameter is given in Fig. 10.

In these calculations no reference is made to the relationship between the length of the arm l and the reduced frequency λ which is treated as an independent variable. It will of course depend upon the actual dimensions of the aerofoil, the inertia of the system and, if applied to aircraft, upon other parts of the airframe contributing mass and stiffness.

It must be noted that the results of this approach towards the dynamic stability with unsteady flow is more correct than the calculations of the preceding sections, since no additional linearisations have had to be assumed. On the other hand it should be emphasized that the unsteady aerodynamic coefficients used are still subject to experimental proof.

8. *Conclusions*.—(*a*) It has been shown that if account is taken of the unsteady flow conditions which exist during the oscillation of an aircraft, the damping may very well be less than would have been expected on the basis of quasi-steady flow theory.

(*b*) If allowance is made for compressibility effects assuming no shock-waves are present, any deterioration in damping associated with the unsteady flow conditions becomes very much worse with increasing Mach numbers.

(*c*) The deterioration in damping is likely to be particularly severe in the case of tailless aircraft or aircraft with short tail arms. The dynamic longitudinal stability of tailless aircraft is particularly affected with forward c.g. positions with respect to the neutral point of the wing. This will generally be the case if some fuselage is present.

(*d*) The frequencies of the aircraft oscillations are not appreciably affected by allowing for unsteady flow conditions.

9. *Future Work*.—This report aims only to give an indication of the probable consequences of the effects of unsteady flow on aircraft stability. The importance of the foregoing conclusions to practically all aircraft with high subsonic speed suggests more thorough investigation of all aspects of the problem. There are four lines along which further research should proceed :

(*a*) Flight research on the dynamic stability of high-speed aircraft.

(*b*) Wind-tunnel or flight measurements on oscillating aerofoils. A simple experiment would be observation of self-excited oscillations of a freely suspended wind vane as investigated theoretically in section 7 of this paper at high speeds.

(*c*) Theoretical analysis on the unsteady compressible flow round wings with finite aspect ratio and sweep. An approach towards a solution of the unsteady flow round bodies of revolution seems also desirable.

(*d*) More comprehensive treatment of the dynamic stability of aircraft with more than two degrees of freedom, and of the problem of auto-stabilisation with unsteady aerodynamic control effectiveness.

If the conclusions of this paper are confirmed the provision of means for artificial dynamic stabilisation of aircraft may prove inevitable in many cases and the development of such means should be urged.

LIST OF SYMBOLS

A	=	b^2/S, aspect ratio
$A_{\alpha(\psi)}$		Damping root
a_0		Two-dimensional lift slope
a_1		Three-dimensional lift slope
b		Wing span
B		Inertia in pitch
$c_{(T, F)}$		Chord of wing (tailplane, fin)
C_L	=	$L/\frac{1}{2}\rho V^2 S$, lift coefficient
C_M	=	$M/\frac{1}{2}\rho V^2 Sc$, pitching-moment coefficient
C_N	=	$N/\frac{1}{2}\rho V^2 Sb$, yawing-moment coefficient
C_y	=	$Y/\frac{1}{2}\rho V^2 S$, side-force coefficient
i	=	$\sqrt{-1}$
i_B	=	B/ml^2, inertia coefficient in pitch
i_c	=	$C/m(b/2)^2$, inertia coefficient in yaw
L		Lift
$l_{(W, F)}$		Distance between the quarter-chord of tailplane (wing, fin) and the c.g.
l_α	=	$\partial C_L/\partial\alpha^*$, lift derivative with respect to α^* (Flutter coefficients)
l_z	=	$\partial C_L/\partial(z/c)$, lift derivative with respect to z (Flutter coefficients)
l_η	=	$\partial C_L/\partial\eta$, lift derivative with respect to η (Flutter coefficients)
m_α	=	$\partial C_M/\partial\alpha^*$, moment derivative with respect to α^* (Flutter coefficients)
m_z	=	$\partial C_M/\partial(z/c)$, moment derivative with respect to z (Flutter coefficients)
m		Mass of the aircraft
M		Pitching moment
M_0		Pitching moment about quarter-chord of an individual aerofoil
N		Yawing moment
q	=	$\dot{\theta}$, rate of pitch
r	=	$\dot{\psi}$, rate of yaw
$S_{(T, F)}$		Area of wing (tailplane, fin)
$T_{\alpha(\psi)}$		Period of the longitudinal (lateral) oscillation
$t_{\alpha(\psi)}$		Damping time of the longitudinal (lateral) oscillation
$\hat{t}$	=	$m/\rho SV$, time unit
v		Lateral velocity component
V		Speed of flight
W		Weight
w		Vertical velocity component

Y		Side force
z		Vertical displacement
α	=	w/V, aerodynamic inclination
α^*		Flutter variable
β	=	v/V, angle of sideslip
γ		Angle of climb
δ	=	T/t, logarithmic decrement
ε		Downwash angle
ε_t		Phase lag angle
η		Control deflection
θ		Altitude in pitch
λ	=	$\omega c/V$, reduced frequency
Λ	=	TV, wavelength of an oscillation
μ_1	=	$m/\rho Sl$, relative density (longitudinal)
μ_2	=	$2m/\rho Sb$, relative density (lateral)
ρ		Air density
χ		Azimuth angle at the flight path
ψ		Attitude in yaw
ω	=	$2\pi/T$, circular frequency

$$m_\alpha = \frac{\partial C_m}{\partial \alpha}\frac{c}{2l}$$

$$\overline{m}_{\dot{\alpha}} = \frac{\partial C_M}{\partial(\dot{\alpha}l/V)}\frac{c}{2l}$$

$$m_q = \frac{\partial C_M}{\partial(ql/V)}\frac{c}{2l}$$

Quasi-steady pitching-moment derivatives

$$m_\theta = \frac{\partial C_M}{\partial \theta}\frac{c}{2l}$$

$$m_{\dot{\theta}} = \frac{\partial C_M}{\partial(\dot{\theta}l/V)}\frac{c}{2l}$$

$$m_\gamma = \frac{\partial C_M}{\partial \gamma}\frac{c}{2l}$$

$$m_{\dot{\gamma}} = \frac{\partial C_M}{\partial(\dot{\gamma}l/V)}\frac{c}{2l}$$

Unsteady pitching-moment derivatives

$$n_v = \frac{\partial C_N}{\partial \beta}$$

$$n_r = \frac{\partial C_N}{\partial(rb/2V)}$$

Quasi-steady yawing-moment derivatives

$$\left.\begin{aligned} n_{\psi} &= \frac{\partial C_N}{\partial \psi} \\ n_{\dot{\psi}} &= \frac{\partial C_N}{\partial(\dot{\psi} b/2V)} \\ n_{\chi} &= \frac{\partial C_N}{\partial \chi} \\ n_{\dot{\chi}} &= \frac{\partial C_N}{\partial(\dot{\chi} b/2V)} \end{aligned}\right\} \text{Unsteady yawing-moment derivatives}$$

$$\left.\begin{aligned} y_v &= \tfrac{1}{2}\frac{\partial C_y}{\partial \beta} \\ y_r &= \tfrac{1}{2}\frac{\partial C_y}{\partial(rb/2V)} \end{aligned}\right\} \text{Quasi-steady side-force derivatives}$$

$$\left.\begin{aligned} y_{\psi} &= \tfrac{1}{2}\frac{C_y}{\partial \psi} \\ y_{\dot{\psi}} &= \tfrac{1}{2}\frac{C_y}{\partial(\dot{\psi} b/2V)} \\ y_{\chi} &= \tfrac{1}{2}\frac{C_y}{\partial \chi} \\ y_{\dot{\chi}} &= \tfrac{1}{2}\frac{C_y}{\partial(\dot{\chi} b/2V)} \end{aligned}\right\} \text{Unsteady side-force derivatives}$$

$$\left.\begin{aligned} z_w &= -\tfrac{1}{2}\frac{\partial C_L}{\partial \alpha} \\ z_q &= -\tfrac{1}{2}\frac{\partial C_L}{\partial(ql/V)} \end{aligned}\right\} \text{Quasi-steady lift derivatives}$$

$$\left.\begin{aligned} z_{\theta} &= -\tfrac{1}{2}\frac{\partial C_L}{\partial \theta} \\ z_{\dot{\theta}} &= -\tfrac{1}{2}\frac{\partial C_L}{\partial(\dot{\theta} l/V)} \\ z_{\gamma} &= -\tfrac{1}{2}\frac{\partial C_L}{\partial \gamma} \\ z_{\dot{\gamma}} &= -\tfrac{1}{2}\frac{\partial C_L}{\partial(\dot{\gamma} l/V)} \end{aligned}\right\} \text{Unsteady lift derivatives}$$

REFERENCES

No.	Author	Title, etc.
1	H. Glauert	The force and moment of an oscillating aerofoil. R. & M. 1242. March, 1929.
2	W. E. Cotter	Summary and analysis of data on damping in yaw and pitch for a number of airplane models. N.A.C.A. Tech. Note 1080. May, 1946.
3	G. Temple	*Modern developments in fluid dynamics.* Vol. III, Chapter IX. Unsteady Motion. A.R.C. 11,745. May, 1949.
4	A. I. Nekrasov	*Wing theory for unsteady motion.* Section 4, Chapter XI, Summary of formulae and bibliography. (Academy of Sciences, U.S.S.R.) Translated by S. W. Skan. A.R.C. 11,795. September, 1948.
5	Frazer, Schade and Dieze	Tables and curves of two-dimensional subsonic aerodynamic derivatives. Unpublished data by Structures Dept., Royal Aircraft Establishment.
6	Th. Schade	Numerische Lösung der Possio'schen Integralgleichung der schwingenden Tragfläche in ebener Unterschallströwung. U. & M. 3209. 1944.
7	K. Krienes and Th. Schade	Theorie der schwingenden Kreisfläche auf potential-theoretischer Grundlage. *Luftfahrtforschung,* Vol. 19. No. 8.
8	W. P. Jones	Aerodynamic forces on wings in non-uniform motion. R. & M. 2117. August, 1945.
9	B. Smilg	The instability of pitching oscillations of an airfoil in subsonic incompressible potential flow. *J. Aero. Sci.* November, 1949.
10	H. Goland	Stick-fixed short-period stability based on the Wagner air forces. Reissner Anniversary Volume. Contributions to applied mechanics. J. W. Edwards and Ann Arbor. Michigan, 1949.

TABLE 1

Derivatives of the Unsteady Aerodynamic Coefficients with respect to λ or λ^2 respectively (Referred to quarter-chord)

Mach number	$\frac{\partial l_{\alpha i}}{\partial \lambda}$	$\frac{\partial l_{zi}}{\partial \lambda}$	$\frac{\partial m_{\alpha i}}{\partial \lambda}$	$\frac{\partial m_{zi}}{\partial \lambda}$	$\frac{\partial l_{zR}}{\partial \lambda^2}$	$\frac{\partial m_{zR}}{\partial \lambda^2}$
0	− 7·12	6·06	−0·76	0	8	0·39
0·5	−12·87	6·90	−1·07	0	12	0·56
0·6	−16·85	7·38	−1·25	0	16	0·71
0·7	−23·86	8·14	−1·58	0·03	21	0·94
0·8	−41·00	10·00	−1·90	0·08	47	1·40

TABLE 2

Real Parts of the Unsteady Aerodynamic Coefficients with Apparent Mass Effect Included

Mach number	λ	$l_{\alpha R}$	l_{zR}	$m_{\alpha R}$	m_{zR}
0	0	6·284	0	0	0
	0·04	6·065	0·0163	0	0·0006
	0·08	5·849	0·0483	0	0·0026
0·5	0	7·256	0	0	0
	0·04	6·906	0·0261	0	0·0009
	0·08	6·566	0·0763	−0·001	0·0037
0·7	0	8·798	0	0	0
	0·04	8·148	0·0445	−0·003	0·0015
	0·08	7·545	0·1261	−0·007	0·0061
0·8	0	10·440	0	−0·010	0
	0·04	9·575	0·100	−0·040	0·0030
	0·08	8·652	0·190	−0·080	0·0049

TABLE 3

Dimensions and Data of the Two Aircraft Considered in the Numerical Example

			Aircraft A	Aircraft B
Wing	area	S	320 ft²	320 ft²
	span	b	40 ft	40 ft
	wing load	W/S	40 lb/ft²	35 lb/ft²
	chord	c	8 ft	8 ft
	arm	l_W	0	2 ft
	aspect ratio	A_W	5	5
μ_1	(ground level)		21·7	57·1
μ_2	(ground level)		26·1	22·85
inertia in yaw		i_c	0·15	0·11
inertia in pitch		i_B	0·12	0·50
Tail	area	S_T	48 ft²	0
	chord	C_T	4 ft	0
	arm	l	24 ft	—
	aspect ratio	A_T	3	—
Fin	area	S_F	24 ft²	24 ft²
	chord	C_F	4 ft	4 ft
	arm	l_F	24 ft	16 ft
	aspect ratio	A_F	1·5	1·5
quasi-steady fuselage derivatives		$(m_w)_{FUS}$	0·050	0·15*
		$(n_v)_{FUS}$	−0·070	−0·045
		$(y_v)_{FUS}$	−0·20	−0·15

* 0·08 for the smaller fuselage.

TABLE 4

Unsteady Derivatives and Stability Coefficients of the Longitudinal Oscillation of the Tailed Aircraft A

Mach number	0	0·5	0·7	0·8
$(m_\theta)_T$	−0·170	−0·192	−0·221	−0·254
$(m_\gamma)_T$	0·177	0·200	0·235	0·289
Σm_θ	−0·120	−0·142	−0·171	−0·204
Σm_γ	0·127	0·150	0·185	0·239
$(m_{\dot\theta})_T$	−0·216	−0·223	−0·222	−0·217
$(m_{\dot\theta})_W$	−0·027	−0·038	−0·057	−0·068
$\Sigma m_{\dot\theta}$	−0·243	−0·261	−0·279	−0·285
$(m_{\dot\gamma})_T$	−0·038	−0·058	−0·101	−0·229
$(m_{\dot\gamma})_W$	0·014	0·020	0·034	0·050
$\Sigma m_{\dot\gamma}$	−0·024	−0·038	−0·067	−0·179
$(z_\theta)_T$	−0·178	−0·205	−0·246	−0·291
$(z_\theta)_W$	−1·88	−2·12	−2·43	−2·78
Σz_θ	−2·06	−2·32	−2·68	−3·07
$(z_\gamma)_T$	0·172	0·196	0·231	0·284
$(z_\gamma)_W$	1·95	2·22	2·62	3·22
$\Sigma_{z\gamma}$	2·12	2·42	2·85	3·50
$(z_{\dot\theta})_T$	−0·216	−0·223	−0·221	−0·205
$(z_{\dot\theta})_W$	0·764	1·380	2·542	4·400
$\Sigma_{z\dot\theta}$	0·548	1·157	2·321	4·195
$(z_{\dot\gamma})_T$	−0·039	−0·058	−0·101	−0·226
$(z_{\dot\gamma})_W$	−0·860	−1·290	−2·260	−5·050
$\Sigma z_{\dot\gamma}$	−0·899	−1·348	−2·361	−5·276
$\overline{m}_{\dot W}$	−0·099	−0·132	−0·187	−0·272
A_α	4·90	5·59	6·52	7·43
B_α	29·5	37·4	49·7	80·0
Λ_α ft	779	687	605	471
λ_W	0·064	0·073	0·083	0·106
λ_T	0·032	0·037	0·042	0·053

TABLE 5

Unsteady Aerodynamic Derivatives and Stability Roots of the Longitudinal Oscillation of the Tailless Aircraft B *with Large Fuselage*

	Mach number	0	0·5	0·7	0·8
$l_W/c = 0{\cdot}10$	m_θ	−0·189	−0·212	−0·245	−0·304
	m_γ	0·195	0·222	0·252	0·296
	$m_{\theta\ FUS}$	0·150	0·173	0·210	0·250
	Σm_θ	−0·039	−0·039	−0·035	−0·054
	Σm_γ	0·045	0·049	0·042	0·046
	$m_{\dot\theta}$	0·018	0·070	0·259	0·707
	$m_{\dot\gamma}$	−0·130	−0·212	−0·373	−1·060
	z_θ	−1·885	−2·115	−2·434	−2·785
	z_γ	1·950	2·220	2·620	3·220
	$z_{\dot\theta}$	2·48	4·36	7·96	13·50
	$z_{\dot\gamma}$	−2·57	−3·86	−6·75	−15·13
	A_α	1·819	1·913	1·734	0·736
	B_α	4·62	4·72	4·32	7·02
	Λ_α	1467	1478	1520	1090
	λ_W	0·034	0·034	0·033	0·046
$l_W/c = 0{\cdot}20$	m_θ	−0·377	−0·424	−0·489	−0·585
	m_γ	0·390	0·445	0·515	0·619
	Σm_θ	−0·227	−0·251	−0·279	−0·335
	Σm_γ	0·240	0·272	0·305	0·369
	$m_{\dot\theta}$	0·136	0·395	0·956	1·906
	$m_{\dot\gamma}$	−0·390	−0·593	−1·850	−2·675
	z_θ	−1·888	−2·120	−2·440	−2·800
	z_γ	1·950	2·220	2·620	3·220
	$z_{\dot\theta}$	1·904	3·660	7·15	12·57
	$z_{\dot\gamma}$	−2·57	−3·86	−6·75	−15·13
	A_α	+1·568	+1·222	+0·200	−2·096
	B_α	26·39	29·42	33·07	42·15
	Λ_α ft	567	535	501	447
	λ_W	0·089	0·094	0·100	0·112

TABLE 6

Unsteady Aerodynamic Derivatives and Stability Roots of the Longitudinal Oscillation of the Tailless Aircraft B *with Small Fuselage*

Mach number	0	0·5	0·7	0·8
m_θ	−0·101	−0·117	−0·142	−0·168
m_γ	0·098	0·111	0·131	0·135
$m_{\theta\ FUS}$	0·080	0·094	0·112	0·130
Σm_θ	−0·021	−0·023	−0·030	−0·038
Σm_γ	0·018	0·017	0·019	0·005
$m_{\dot\theta}$	−0·132	−0·143	−0·129	+0·041
$m_{\dot\gamma}$	−0·003	−0·013	−0·035	−0·306
z_θ	−1·885	−2·115	−2·434	−2·785
z_γ	1·950	2·220	2·620	3·220
$z_{\dot\theta}$	2·20	4·04	7·55	13·04
$z_{\dot\gamma}$	−2·58	−3·87	−6·77	−15·15
A_α	2·302	2·666	3·218	4·14
B_α	2·43	2·71	3·61	5·64
Λ_α	2720	2990	2840	2470
λ_W	0·0185	0·0168	0·0176	0·0203

$l_W/c = 0{\cdot}05$ corresponding to c.g. at 20 per cent of the wing chord.

TABLE 7

Unsteady Aerodynamic Derivatives and Stability Coefficients of the Lateral Oscillation of the Long Tail A *and Short Tail Version* B

	Mach number	0	0·5	0·7	0·8
A	$(n_\psi)_F$	−0·106	−0·121	−0·142	−0·167
	$(n_\chi)_F$	0·105	0·120	0·142	0·174
	Σn_ψ	−0·036	−0·051	−0·072	−0·094
	Σn_χ	0·035	0·050	0·072	0·104
	$n_{\dot\psi}$	−0·102	−0·100	−0·087	−0·067
	$n_{\dot\chi}$	−0·028	−0·042	−0·073	−0·162
	$(y_\psi)_F$	+0·089	+0·102	0·120	0·142
	$(y_\chi)_F$	−0·088	−0·100	−0·118	−0·145
	Σy_ψ	0·289	0·302	0·320	0·342
	Σy_χ	−0·288	−0·300	−0·318	−0·345
	$y_{\dot\psi}$	0·085	0·083	0·072	0·055
	$y_{\dot\chi}$	0·023	0·035	0·061	0·136
	A_ψ	0·974	0·977	0·892	0·816
	B_ψ	6·45	8·96	12·53	16·60
	Λ_ψ	1318	1114	936	811
	λ_F	0·019	0·022	0·027	0·030
B	$(n_\psi)_F$	−0·070	−0·079	−0·092	−0·108
	$(n_\chi)_F$	0·070	0·080	0·095	0·116
	Σn_ψ	−0·025	−0·034	−0·047	−0·063
	Σn_χ	+0·025	0·035	0·050	0·071
	$n_{\dot\psi}$	−0·040	−0·035	−0·021	+0·001
	$n_{\dot\chi}$	−0·018	−0·028	−0·049	−0·109
	$(y_\psi)_F$	+0·088	0·099	0·117	0·136
	$(y_\chi)_F$	−0·088	−0·100	−0·118	−0·145
	$\Sigma_\psi y$	0·238	0·249	0·267	0·286
	Σy_χ	−0·238	−0·250	−0·268	−0·295
	$y_{\dot\psi}$	0·050	0·043	0·025	−0·003
	$y_{\dot\chi}$	0·023	0·035	0·061	0·136
	A_ψ	0·604	0·564	0·457	0·285
	B_ψ	5·26	7·15	9·94	13·40
	Λ_ψ	1265	1080	912	785
	λ_F	0·020	0·023	0·028	0·052

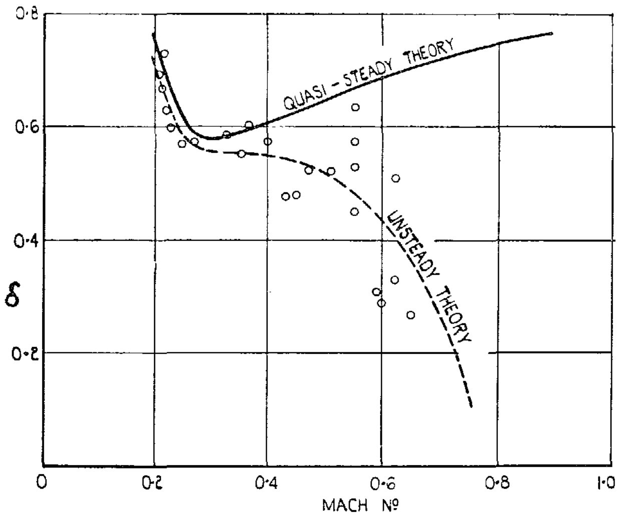

FIG. 1. Logarithmic decrement δ of the directional oscillation of the *Meteor* against Mach number. Comparison between flight-test results (o) and Quasi-steady theory and unsteady theory.

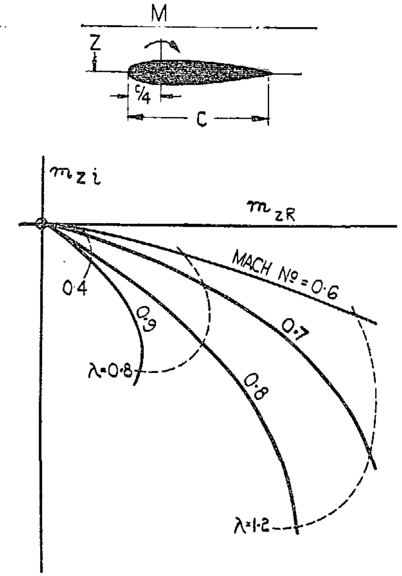

FIG. 4. Unsteady moment coefficient m_z due to a translatory oscillation of an aerofoil against frequency parameter λ and Mach number.

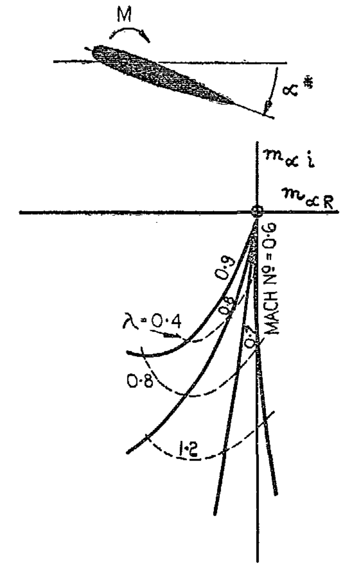

FIG. 5. Unsteady moment coefficient m_α due to an angular oscillation of an aerofoil against frequency parameter λ and Mach number.

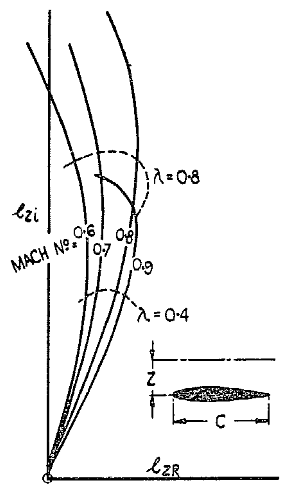

FIG. 2. Unsteady lift l_z due to a translatory oscillation of an aerofoil with the amplitude (z/c) against frequency λ and Mach number.

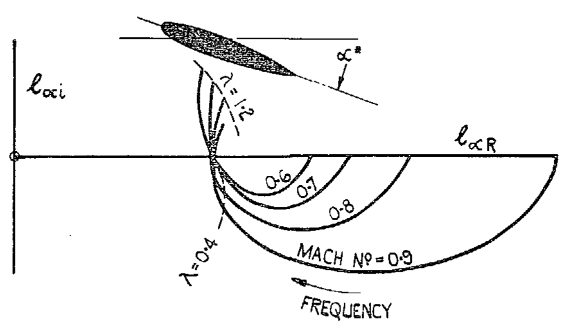

FIG. 3. Unsteady lift l_α due to an angular oscillation of an aerofoil about its quarter-chord line with the amplitude α^* against frequency λ and Mach number.

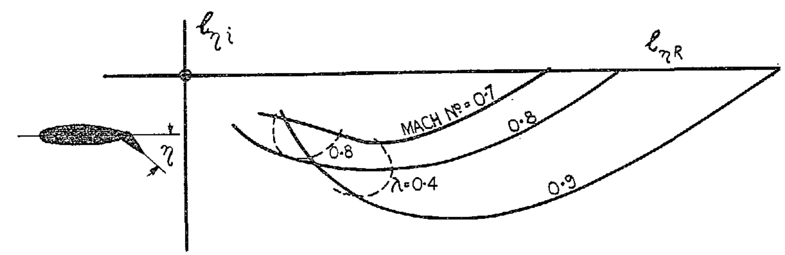

FIG. 6. Unsteady lift coefficient l_η due to a harmonic flap deflection with the amplitude η against frequency parameter λ and Mach number (flap chord c_η 20 per cent of the wing chord c).

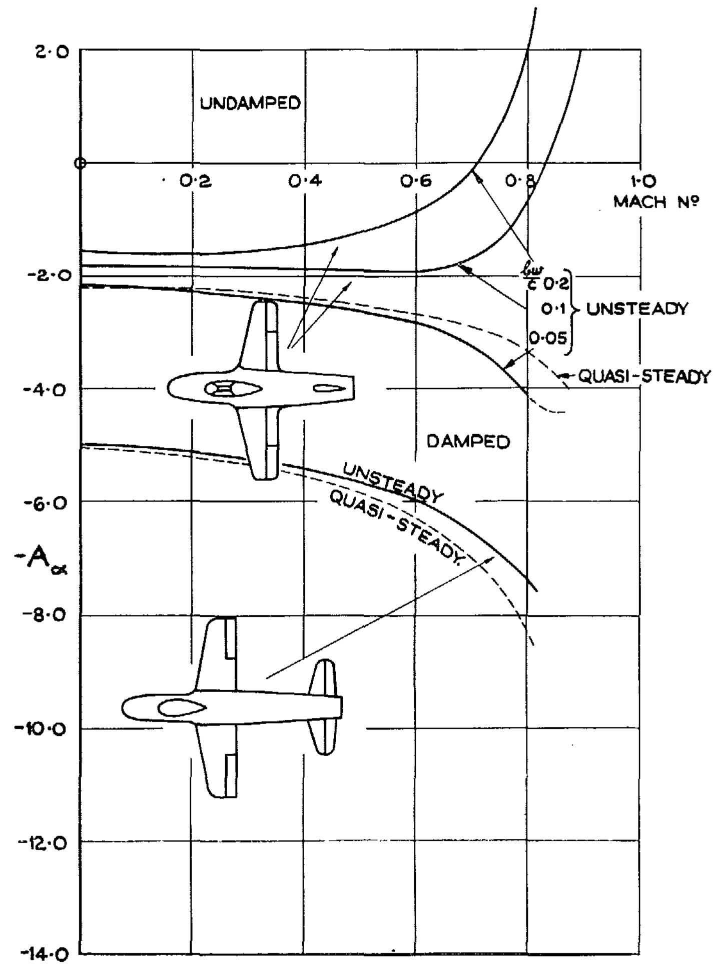

FIG. 7. Damping root A_α of the longitudinal oscillation of two aircraft as affected by unsteady flow.

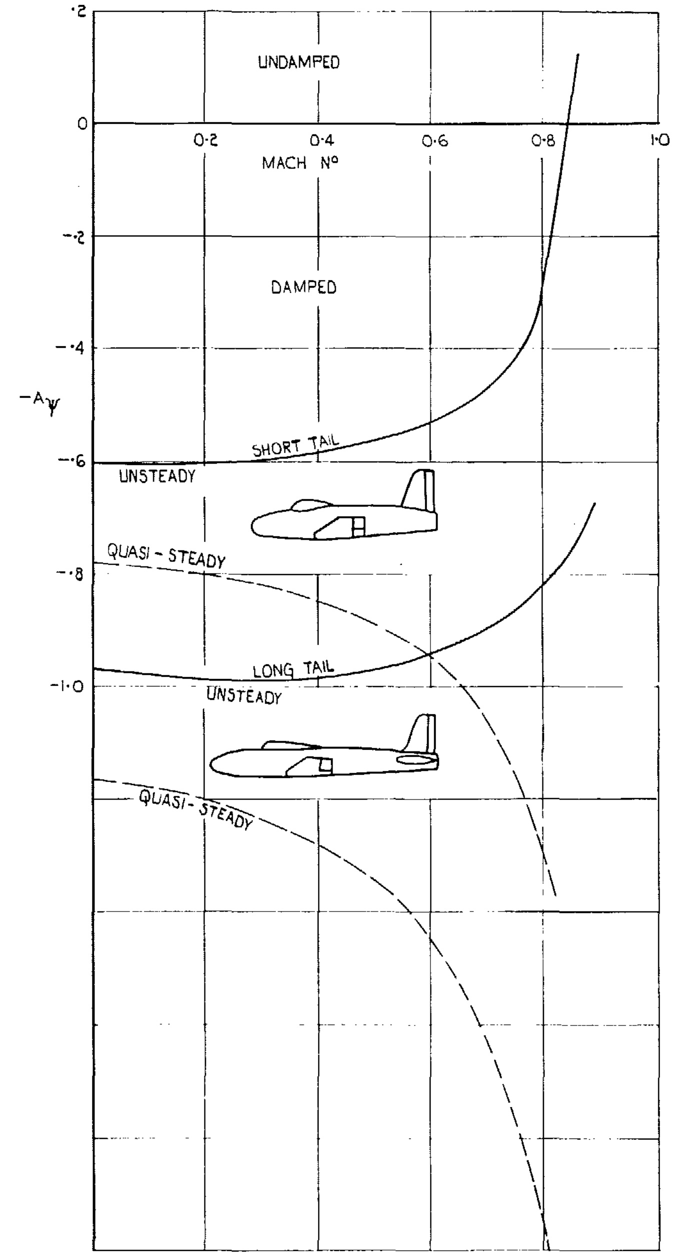

FIG. 8. Damping root A_ψ of the directional oscillation of two aircraft as affected by unsteady flow.

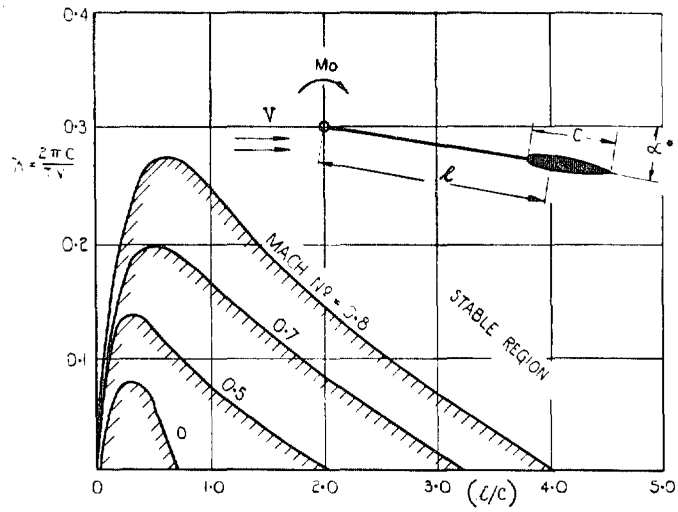

FIG. 9. Stability boundaries of the oscillation of a wind vane against Mach number. Arm of the aerofoil l and reduced frequency λ.

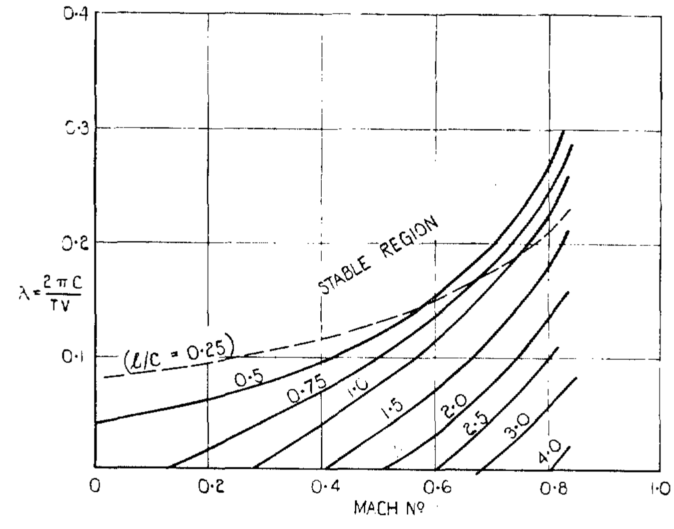

FIG. 10. Stability boundaries of the oscillation of a wind vane (cross-plotting from Fig. 9).

(61801) Wt. 17/680 K.9 9/54 Hw PRINTED IN GREAT BRITAIN

Publications of the Aeronautical Research Council

ANNUAL TECHNICAL REPORTS OF THE AERONAUTICAL RESEARCH COUNCIL (BOUND VOLUMES)

1936 Vol. I. Aerodynamics General, Performance, Airscrews, Flutter and Spinning. 40*s.* (41*s.* 1*d.*)
Vol. II. Stability and Control, Structures, Seaplanes, Engines, etc. 50*s.* (51*s.* 1*d.*)

1937 Vol. I. Aerodynamics General, Performance, Airscrews, Flutter and Spinning. 40*s.* (41*s.* 1*d.*)
Vol. II. Stability and Control, Structures, Seaplanes, Engines, etc. 60*s.* (61*s.* 1*d.*)

1938 Vol. I. Aerodynamics General, Performance, Airscrews. 50*s.* (51*s.* 1*d.*)
Vol. II. Stability and Control, Flutter, Structures, Seaplanes, Wind Tunnels, Materials. 30*s.* (31*s.* 1*d.*)

1939 Vol. I. Aerodynamics General, Performance, Airscrews, Engines. 50*s.* (51*s.* 1*d.*)
Vol. II. Stability and Control, Flutter and Vibration, Instruments, Structures, Seaplanes, etc. 63*s.* (64*s.* 2*d.*)

1940 Aero and Hydrodynamics, Aerofoils, Airscrews, Engines, Flutter, Icing, Stability and Control, Structures, and a miscellaneous section. 50*s.* (51*s.* 1*d.*)

1941 Aero and Hydrodynamics, Aerofoils, Airscrews, Engines, Flutter, Stability and Control, Structures. 63*s.* (64*s.* 2*d.*)

1942 Vol. I. Aero and Hydrodynamics, Aerofoils, Airscrews, Engines. 75*s.* (76*s.* 3*d.*)
Vol. II. Noise, Parachutes, Stability and Control, Structures, Vibration, Wind Tunnels. 47*s.* 6*d.* (48*s.* 7*d.*)

1943 Vol. I. Aerodynamics, Aerofoils, Airscrews. 80*s.* (81*s.* 4*d.*)
Vol. II. Engines, Flutter, Materials, Parachutes, Performance, Stability and Control, Structures. 90*s.* (91*s.* 6*d.*)

1944 Vol. I. Aero and Hydrodynamics, Aerofoils, Aircraft, Airscrews, Controls. 84*s.* (85*s.* 8*d.*)
Vol. II. Flutter and Vibration, Materials, Miscellaneous, Navigation, Parachutes, Performance, Plates and Panels, Stability, Structures, Test Equipment, Wind Tunnels. 84*s.* (85*s.* 8*d.*)

Annual Reports of the Aeronautical Research Council—

1933–34	1*s.* 6*d.* (1*s.* 8*d.*)	1937	2*s.* (2*s.* 2*d.*)
1934–35	1*s.* 6*d.* (1*s.* 8*d.*)	1938	1*s.* 6*d.* (1*s.* 8*d.*)
April 1, 1935 to Dec. 31, 1936	4*s.* (4*s.* 4*d.*)	1939–48	3*s.* (3*s.* 2*d.*)

Index to all Reports and Memoranda published in the Annual Technical Reports, and separately—

April, 1950 - - - - R. & M. No. 2600. 2*s.* 6*d.* (2*s.* 7½*d.*)

Author Index to all Reports and Memoranda of the Aeronautical Research Council—

1909–1949. R. & M. No. 2570. 15*s.* (15*s.* 3*d.*)

Indexes to the Technical Reports of the Aeronautical Research Council—

December 1, 1936 — June 30, 1939.	R. & M. No. 1850.	1*s.* 3*d.* (1*s.* 4½*d.*)
July 1, 1939 — June 30, 1945.	R. & M. No. 1950.	1*s.* (1*s.* 1½*d.*)
July 1, 1945 — June 30, 1946.	R. & M. No. 2050.	1*s.* (1*s.* 1½*d.*)
July 1, 1946 — December 31, 1946.	R. & M. No. 2150.	1*s.* 3*d.* (1*s.* 4½*d.*)
January 1, 1947 — June 30, 1947.	R. & M. No. 2250.	1*s.* 3*d* (1*s.* 4½*d.*)
July, 1951.	R. & M. No. 2350.	1*s.* 9*d.* (1*s.* 10½*d.*)

Prices in brackets include postage.

Obtainable from

HER MAJESTY'S STATIONERY OFFICE

York House, Kingsway, London, W.C.2; 423 Oxford Street, London, W.1 (Post Orders: P.O. Box 569, London, S.E.1); 13a Castle Street, Edinburgh 2; 39, King Street, Manchester 2; 2 Edmund Street, Birmingham 3; 1 St. Andrew's Crescent, Cardiff; Tower Lane, Bristol 1; 80 Chichester Street, Belfast, or through any bookseller

S.O. Code No. 23-2904

R. & M. No. 2904